Sigma J Eng Nat Sci, Vol. 44, No. 3, pp. 1561–1571, June, 2026

Sigma Journal of Engineering and Natural Sciences
Web page info: https://sigma.yildiz.edu.tr
DOI: 10.14744/sigma.2026.2052

Research Article

Study of the physical structure and performance of vertical wind turbines evaluated by bio-mimicry Dipterocarpus alatus, Part 1

Montri LUNGCHAVANON[1,2,*], Kuaanan TECHATO[3], Woradej MANOSROI[4], Ekawat RATCHAİ[1], Suratsavadee Koonlaboon KORKUA[5]

[1]*Wind Energy and Energy Storage Systems Centre (WEESYC), Faculty of Environmental Management, Prince of Songkla University, Hat Yai, Songkhla, 90110, Thailand*
[2]*Centre of Excellence in Materials Engineering (CEME), Faculty of Engineering, Prince of Songkla University, Hat Yai, Songkhla, 90110, Thailand*
[3]*Department of Sustainable Energy Management, Faculty of Environmental Management, Prince of Songkla University, Hat Yai 90110, Thailand*
[4]*Department of Mechanical Engineering, Faculty of Engineering, Chiang Mai University, 50200, Thailand*
[5]*School of Engineering and Technology Academic Building 4, Walailak University, 222 Thaiburi, Thasala District Nakhon Si Thammarat, 80160, Thailand*

ARTICLE INFO

Article history
Received: 06 Juney 2024
Revised: 23 July 2024
Accepted: 07 February 2025

Keywords:
Biomimicry; Dipterocarpus Alatus; Low Wind Speed; VAWTs; Wind Energy

ABSTRACT

The design of the blades of wind turbines can take inspiration from biomimicry techniques. The survival of natural designs through natural selection acts as the model. One example is the case of Dipterocarpus alatus, which has a "flying flower" component for plant propagation. This investigation studied the characteristics of Dipterocarpus alatus in terms of its geometrical properties for use in vertical axis wind turbine (VAWT) blades. A biological method that involves designing blades that mimic the shape of the flying flower was adopted since the geometric features of flying flowers allow them to generate lift with relatively little wind. This study involves the examination of VAWTs. The wind turbine blades were designed to achieve optimum rotational speed (RPM) in low-speed wind environments by studying the characteristics of Dipterocarpus alatus in terms of blade geometry, blade characteristics, number of blades, angle, and aspect ratio (AR) in a wind tunnel at wind speeds of 1 to 10 m/s. The most effective VAWT model was found to comprise 3 Blades: AR =1.5, 120° Twist, 30° Attack, with a cut-in wind speed of 1.75 m/s. This configuration offers low cost when compared with the 4-blade alternative. The results of this study indicate that a wind turbine with specific conditions is suitable for the development of small wind turbines.

Cite this article as: Lungchavanon M, Techato K, Manosroi W, Ratchai E, Korkua SK. Study of the physical structure and performance of vertical wind turbines evaluated by bio-mimicry Dipterocarpus alatus, Part 1. Sigma J Eng Nat Sci 2026;44(3):1561–1571.

***Corresponding author.**
*E-mail address: montri.su@psu.ac.th

This paper was recommended for publication in revised form by Editor-in-Chief Ahmet Selim Dalkilic

Published by Yıldız Technical University Press, İstanbul, Turkey

INTRODUCTION

Wind energy is absolutely free to use and available everywhere around the world. It releases no pollution into the atmosphere after consumption. Because the use of wind energy can efficiently decrease the consumption of fossil energies while reducing greenhouse gas emissions, it is presently receiving more attention than ever before to address the situation of the energy crisis [1-3]. The low speed wind turbine is currently the hot issue for harvesting power from the wind. A wind turbine can be classified based on the alignment of its rotation axis, which are called either horizontal axis wind turbines (HAWTs) or vertical axis wind turbine (VAWTs). Nowadays, HAWTs are installed for electricity production globally in large-scale commercial wind power stations, both offshore and onshore [4-6]. There are two main types of VAWTs that are used, including drag force (Savonius) and lift force (Darrieus) [7]. Additionally, VAWTs are clearly popular due to the following advantages [3]: (1) Easier construction and design, enhanced safety for immigrating birds, lower noise emission; (2) Lower maintenance costs due to the drive train including the gearbox, generator and beak that are placed near the ground; (3) Lower manufacturing costs for the duplication of the airfoil design in VAWT blades; (4) Independence from the wind direction because of the low cost and troublesome yaw system that is required.

Micro-wind turbines are gaining interest for placement in urban areas. However, the turbulence of the wind flow needs to be investigated as it is major feature of the air flow in an environment based on the turbulence generated by many properties such as high intensity, and sizeable velocity fluctuations with large vertical components due to the existence of buildings in a city. The wind direction in urban areas changes easily and affects the poor performance of all types of wind turbines [8]. Nevertheless, recent development of VAWTs revealed the performance of this turbine could be enhanced with higher turbulence intensity for a homogeneous isotopic turbulence flow. Further, it may be a better option than HAWTs when applied in urban areas [9]. Moreover, the design for combining many VAWTs to be wind farm with tree structure can be harvested electricity power and beautiful wind turbine [10, 11]. Therefore, the VAWT can be continuously developed for the micro-wind turbines.

Based on biomimicry, the pectoral fins belong to humpback whales that helped as the general for the aerodynamic idea of leading edge tubercles (LET). To advance their swimming higher efficiency, humpback whales have operated perfectly a series of tubercles or bumps along the leading edge of their fins. These tubercles fabricat small vortices on the surface of the pectoral fin that lessen drag and energize the flow [12]. Geometry plant leaf optimizations simulated by Liu et al [13], demonstration of wind blades based on the plant leaf structure performed better structural and mechanical properties such as the static strength, stiffness, and fatigue life compared to the general structures [14]. DTU Wind was indicated which basically all typical wind turbine blade degradation mechanisms such as buckling, coating detachment, trailing edge failure, spar cap/shell adhesive joint degradation. It have revealed their roots in interface degradation. There was development of biomimicry inspired dual-mechanism-based interface adhesives that served combining mechanical interlocking of fibers and chemical adhesion that possible adhesive joint separating parts for re-use of the blade parts [15].

The main component of the VAWT wind turbine is the blades, which should be investigated higher efficiency. The biological approach has been used to design blades that mimic the shape of triplaris samara seeds and maple seeds, which cause the geometrical properties to fabricate typical lift force [16]. These flying flowers produce stable leading-edge vortices (LEV) which boost the lift force while descending [17]. Although the blades of the wind turbine cannot be directly descending, it can duplicate the geometry of the wing part of the seeds and form them into blades to increase the lift produced by the VAWT with higher efficiency. The LEV can be evoked near the base of the wing that should be reliant upon the geometry of the wind, angle of attack and Reynolds number [17]. Moreover, Diptero-carpus alatus is the one of flying flowers that can produce lift force that has been determined for the terminal velocity of the seeds [18].

This investigation studied the characteristics of Diptero-carpus alatus in terms of its geometrical properties for use in VAWT blades. The condition of blades were changed, including the number of blades, angle and Aspect Ratio (AR). The airfoil of Diptero-carpus alatus was tested by a wind tunnel at 1-10 m/s wind speeds to compare revolution per minute (rpm), and the action of starting up of turbine (Cut in). Acrylic materials were used to form the VAWT blades.

MATERIALS AND METHODS

Materials

The small wind tunnel was designed to investigate the original Diptero-carpus alatus flower aerodynamics. The small wind tunnel was produced from acrylic materials with 0.003 m thickness and 3.8 m length of tunnel. The contents for 3 parts of the wind tunnel are shown in Figure 1 (a). Part number 1 shows the 0.8 m length square-based pyramid shape that is connected with 0.5 x 0.5 m diameter in the front and the 0.3 x 0.3 m diameter connected honeycomb (hole with 0.002 m diameter) to generate the smooth air flow. Part number 2 shows the 2 m length longer cube shape that is combined 0.3 x 0.3 m diameter and Diptero-carpus alatus flower installed at the middle side, which composes the mini shaft and bearings. Part number 3 shows the 1.0 m length square-based pyramid shape that is connected to 0.6 x 0.6 diameter fan section and 0.3 x 0.3 diameter connected

to the longer length cube shape. The fan produced wind speed from 0-6 m/s using a 1 hp motor that sucks wind flow from part number 1 of the tunnel. Figure 1 (b) shows the installation of an anemometer for measuring wind speed and a tachometer for measuring the revolution of the sample. The anemometer used GM8903 Hot Wire (Resolution: 0.1°C, 0.001m/s) from Shenzhen, China. The tachometer used Digital Photo DT-2234C+ (Resolution: 0.1 rpm) from Shenzhen, China.

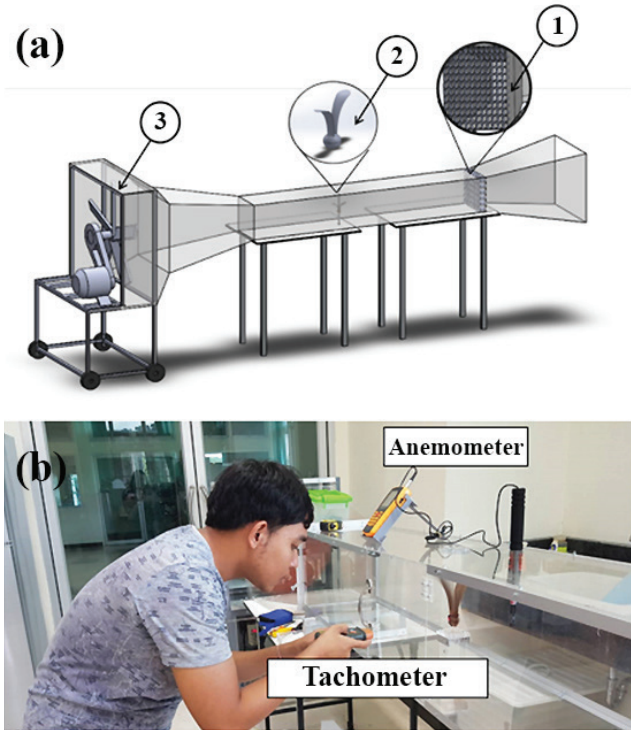

Figure 1. A small wind tunnel used to investigate the original Diptero-carpus alatus flower aerodynamics showing (a) the structure of the small wind tunnel and (b) the installation of an anemometer to measure wind speed and a tachometer to measure the revolution of the sample.

Figure 2 shows the wind tunnel used to investigate the properties of the VAWT blades. The wind tunnel contained a 0.002 thickness metal sheet, 4.2 m length and 1.2 x 1.2 m diameter. The wind tunnel can be used for investigation of 12 sections. 1) The blade model was fabricated from an acrylic sheet 0.003 m in thickness that was designed from the Diptero-carpus alatus flower shape. 2) The shaft and screws can be adjusted and supported by the arm stick and circle plate. The screw at the shaft and arms stick were scaled for the varied angles of VAWTs blades and the circle plate was scaled for the varied degrees of VAWTs blades, as shown in Figure 3. 3) The honeycomb (holes with 0.003 m diameter) was 1.2 x 1.2 m in diameter that controlled smooth airflow. 4) The 5 fans produced wind speeds of 1-10 m/s, which used 1 hp induction motors. 5) The electrical controller circuit used a 5kW inverter for controlling 5 motor induction generated 1-10 m/s wind speed. 6) The anemometer for measuring wind speed used UNI-T UT363 ranging between 0-30m/s. 7) The torque meter for measuring torque force used DRBK-A 0 with a range of (1-100 Nm). 8) The tachometer for measuring revolution used Digital Photo DT-2234C+ (Resolution: 0.1 rpm). 9) The mechanical load of VAWT wind turbine used Drum brake. 10) Wind inlet of the tunnel. 11) Wind outlet of the tunnel.

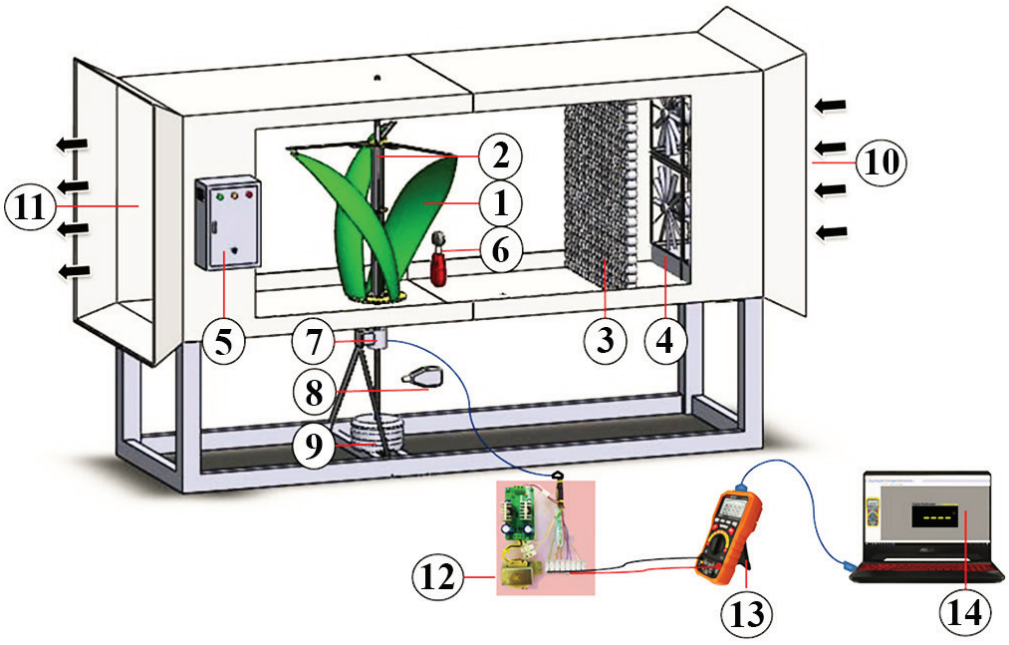

Figure 2. Wind tunnel used to investigate the properties of VAWT blades.

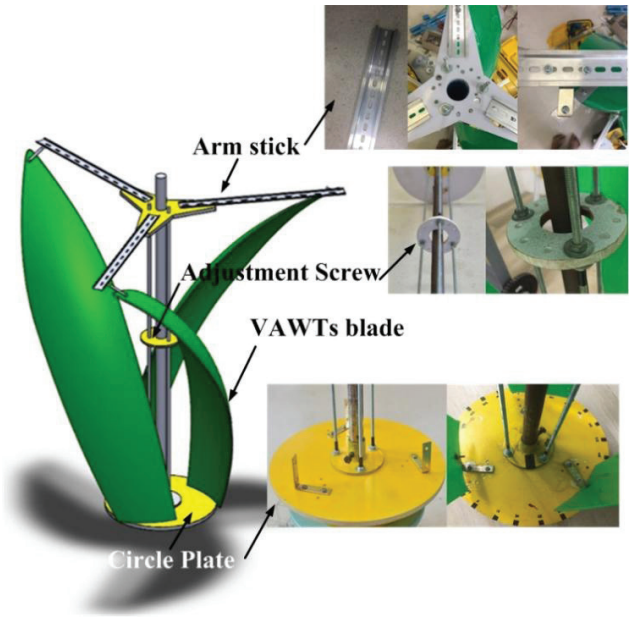

Figure 3. VAWT blade based on Diptero-carpus alatus flower that can be adjusted for blade angles.

12) The $12V_{DC}$ power supply for torque meter. 13) Digital multimetre (PM8236) for measuring the signal from the torque meter and transform to record on a laptop computer. 14) Laptop computer (ASUS TUF Gaming FX505DT) for recorded torque values.

Experimental Blade Design

Figure 4 shows the original Diptero-carpus alatus flower used to fabricate the VAWTs blade. Diptero-carpus alatus grows from March-April every year, and the flowers are harvested from Kuen-Mahachai Village, KuenSri district, Nasan canton, Surat-Thani, Thailand. The Diptero-carpus alatus flower must be a perfectly selected seed. Lacquer was sprayed on the flower against the decadent flower, which increased the strength of the flower when operated in the experiment. Figure 4 (a) shows the experiment of the Diptero-carpus alatus flower installed in a small wind tunnel, and Figure 4 (b) shows the experiment of the upside-down Diptero-carpus alatus flower installed in a small wind tunnel.

Figure 5 shows the duplication of Diptero-carpus alatus flower using grid paper with 1 mm resolution. Figure 5 (a) shows the Diptero-carpus alatus flower deposited on the grid paper that can make the position of the curve inside and the physical curvature of the flower. Figure 5 (b)

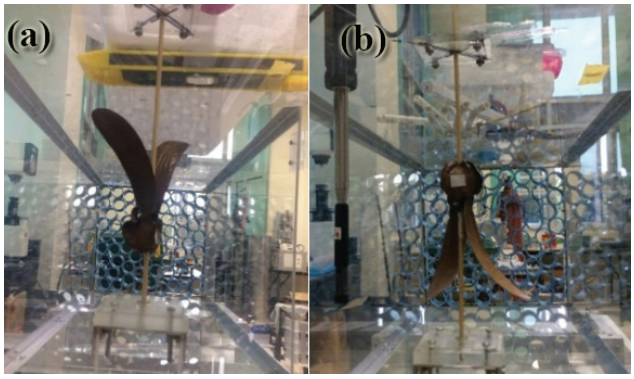

Figure 4. Original Diptero-carpus alatus flower for fabricating the VAWTs blade. (a) The Diptero-carpus alatus flower installed in a small wind tunnel; (b) The upside-down Diptero-carpus alatus flower installed in a small wind tunnel.

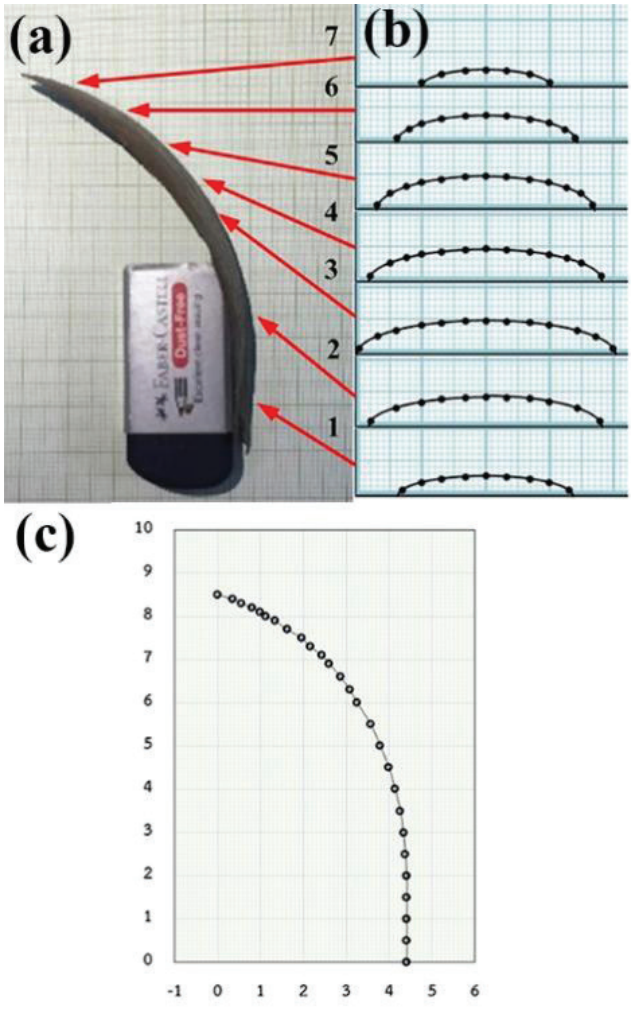

Figure 5. Duplication of Diptero-carpus alatus flower using grid paper with 1 mm resolution, with (a) showing the Diptero-carpus alatus flower deposited on the grid paper, (b) showing the curve inside Diptero-carpus alatus flower with different positions at 1 to 7, and showing the width of Diptero-carpus alatus flower, (c) showing the physical curvature of Diptero-carpus alatus flower.

shows the scale of the width of the flower, which was in the range of 40 mm maximum, while the curve exhibited inside ranged up to 5 mm maximum, which was measured from 7 positions of the Diptero-carpus alatus flower. Figure 5 (c) shows the physical curvature of the Diptero-carpus alatus flower. The width was 45 mm maximum and height was 85 mm maximum.

The VAWT blade was duplicated from the original Diptero-carpus alatus flower to be the scale shown in Figure 5, after which the scale was expanded 100 times using an acrylic sheet, thus forming a curvature as a procedure, as shown in Figure 6. Figure 6 also shows the procedure for forming the VAWT blade that used the acrylic sheet materials. The mould fabricated from Expandable Polystyrene (EPS) is exhibited in Figure 6 (a) with foam materials, which easily produced a curvature on the mould, as shown in Figure 6 (b). The surface of the mould should be stronger for compaction and high temperature than coated Polyester putty cream, as shown in Figure 6 (c). The acrylic sheet was shaped following the design after being heated in a furnace until the sheet was soft, which was then deposited in the mould, as shown in Figure 6 (d). The soft acrylic sheet was compacted by 2 moulds that could control the shape under design and then left for more than 15 minutes to form the saturated acrylic sheet, as shown in Figure 6 (e-f).

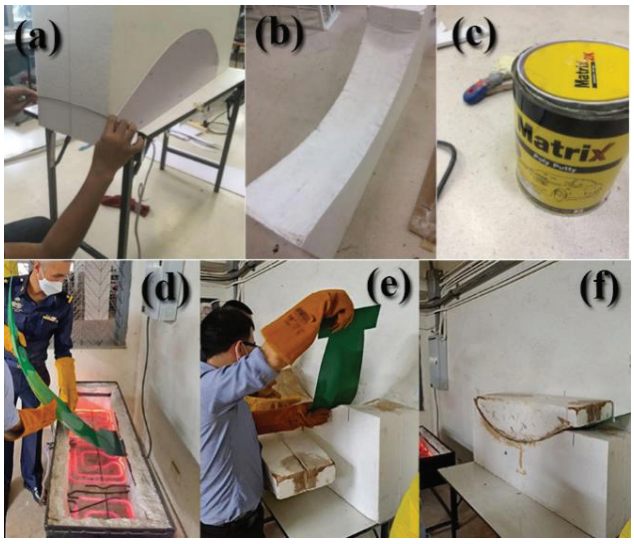

Figure 6. Procedure for forming a VAWT blade. (a) The mould for forming the VAWT blade used Expandable Polystyrene (EPS) foam materials. (b) Producing a curve of VAWT blade based on the design. (c) Polyester putty cream coated on the mould with a stronger surface. (d) Acrylic materials were shaped for the VAWT blade that was heated in a high-temperature furnace. (e) After the Acrylic VAWT blade is heated, it should be soft for easy forming. (d) Compaction of soft Acrylic VAWT blade in the EPS form mould.

Figure 7 shows the parameters for the shape of the fruit and its sepals using dried fruit and wings from the Diptero-carpus alatus. Figure 7 also reveals the blade element in the plane perpendicular to the wing span. Here, ϕ is the angle of the relative wind, α is the angle of attack, L and D are the lift and drag components, respectively. F_N exhibits the vertical forces resulting from F_L and F_D. The camber profile is declarative by the curvature of the blade element. The angular frequency is provided by $\theta = 2\pi f$, where f is the rotational frequency [18]. While a vertical motion of Diptero-carpus alatus depends on the components of life force F_L, drag force F_D and the gravitational force F_G. The magnitude of F_L and F_D on the Diptero-carpus alatus can proportional to life and drag coeffients, C_L and C_D, representively. Thereforce, it can be combined the total forces as shown in Equation (1).

$$|F_G + F_L + F_D| = -mg + \lambda v^2 \quad (1)$$

Where v is the relative wind at the blade and a constant λ, m is mass and g is acceleration due to gravity as shown in Equation (2)

$$\lambda = \tfrac{1}{2}\rho A (C_L + C_D) \quad (2)$$

Where A is the area of the blades of Diptero-carpus alatus and ρ is the air density (approximately 1.225 kg/m^3). Particularly, the drag and life coefficients depend on the blades of Diptero-carpus alatus's angle of attack α that based on C_L (α) and C_D (α)[18].

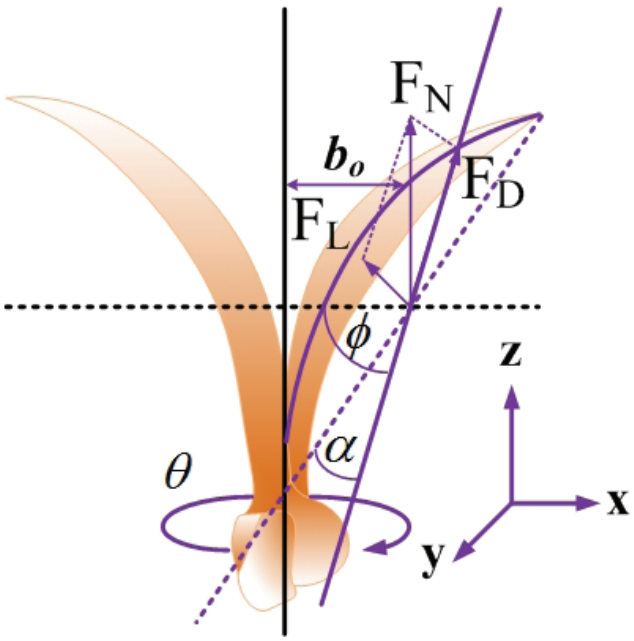

Figure 7. The shape of the seed and its sepals using dried fruit and wings from the Dipterocarpus alatus [18].

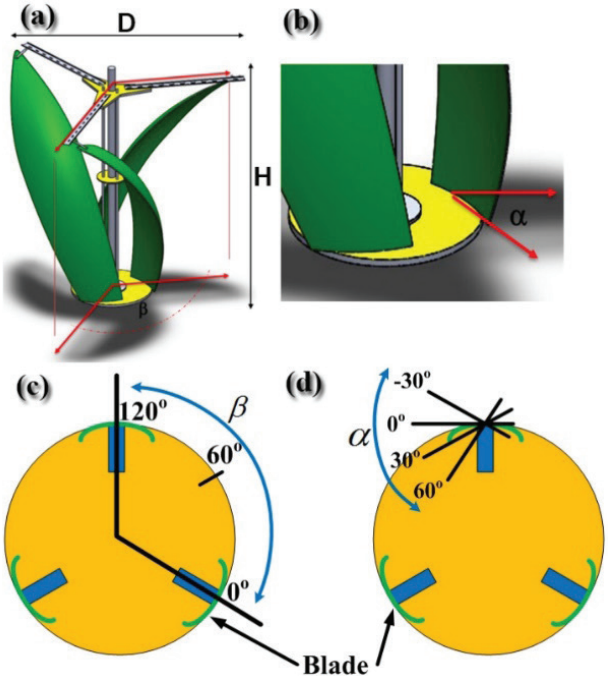

Figure 8. Variation of aspect ratio (AR), β angle, α angle; (a) shows the ratio of AR can be varied by D and H length, representing the β angle between blades; (b) shows the α angle of each blade.

RESULTS AND DISCUSSION

A schematic diagram illustrating the morphology of the Dipterocarpus alatus seed during motion is shown in Figure 9. Five experimental cases were examined, with each case having different blade angles consisting of the different angle configurations used in this investigation. The airflow conditions supplied were the same for each case when considering the attack angles and cone angles of the five samples as shown in Table 3 (The five Dipterocarpus alatus sample cases are represented as $D_{1\text{-}5}$).

Five experimental cases were examined, with each case having different blade angles, consisting of the different

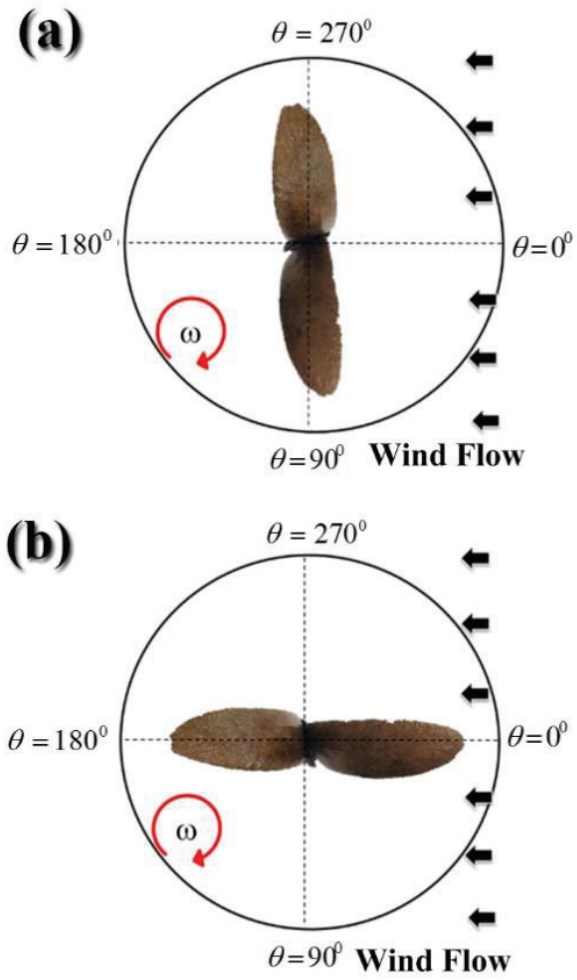

Figure 9. Wind blade angle of dipterocarpus alatus.

angle configurations used in this investigation. The airflow conditions supplied were the same for each case. The comparison of rotational speed (RPM) and wind speed (m/s) discussed in this section is shown in Figure 10.

The plots of rotational speed (RPM) against wind speed (m/s) ranging from 1 m/s to 6 m/s are shown in Figure 10,

Table 1. Blade parameters

Structure of VAWT	(Number of blades)		
	2	3	4
Height (H)	0.9 m	0.9 m	0.9 m
Dimension (D)	0.9 and 0.6 m	0.9 and 0.6 m	0.9 and 0.6 m
Twist Angle, (b)	0°, 60° and 120°	0°, 60 and 120°	0° and 60°
Attack Angle, (a)	-30°, 0°, 30°, 60° and 90°	-30°, 0°, 30°, 60° and 90°	-30°, 0°, 30°, 60° and 90°
Thickness	0.003 m		
Materials	Acrylic		

Table 2. The experiment parameter

	Number of Blades			AR, (Aspect Ratio)		Twist angle, (b)			Attack angle, (a)				
	2	3	4	1.5	1.0	0	60	120	-30	0	30	60	90
VAWT Models	•	-	-	-	-	-	-	-	-	-	-	-	-
		•			•	•			•				
		•			•	•				•			
		•			•	•					•		
		•			•		•			•			
		•			•		•				•		
		•			•		•					•	
		•			•			•			•		
		•			•			•				•	
		•			•			•					•
		•		•		•			•				
		•		•		•				•			
		•		•		•					•		
		•		•			•			•			
		•		•			•				•		
		•		•			•					•	
		•		•				•			•		
		•		•				•				•	
		•		•				•					•
			•		•	•			•				
			•		•	•				•			
			•		•	•					•		
			•	•			•			•			
			•	•			•				•		
			•	•			•					•	

*** Make: 2 blades can stop the rotation when the blades of alignment are at 0°, 90°, so there were no more experiments.

Table 3. Attack angles and cone angles of the five samples; A and B were the two blades which were twisted at attack angles (a) and cone angles (f) as shown in Figure 7.

Samples	Attack angles, α (Degree)		Cone angles, ϕ (Degree)		Direction
	A	B	A	B	
D1	-13.432	-13.067	31.465	23.798	Counter Clockwise
D2	12.702	18.845	34.715	30.179	Clockwise
D3	21.040	22.630	30.290	30.742	Clockwise
D4	-18.202	-25.932	24.426	24.228	Counter Clockwise
D5	13.378	18.442	36.821	37.903	Clockwise

with a total of five different samples used. All the patterns were observed to form a linear graph against increasing wind speed. Wind speed influences the rotational speed of the shaft and thus the power production of a wind turbine [14]. The higher the wind speed, the greater the shaft speed generated [14, 15]. In Figures 10(a) to 10(e), sample D Normal wind turbines start rotating at a lower speed than sample D Upside down wind turbines. This can be

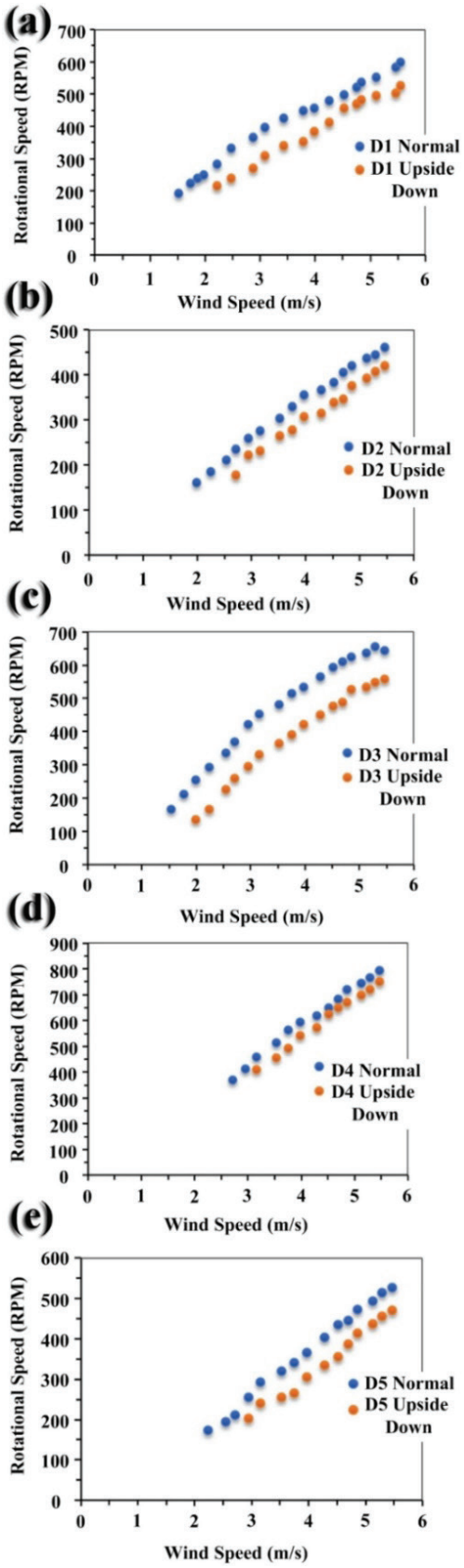

Figure 10. The rotational speed of (RPM) performance against wind speed (m/s) for (a) sample D1, (b) sample D2, (c) sample D3, (d) sample D4, and (e) sample D5.

seen from the rotational speed produced by the sample D Normal turbine, which is higher than the sample D Upside down. When the wind speed is 1.5 m/s, the rotors for the D1 Normal and D3 Normal type wind turbines have started to spin. Conversely, Figure 10(d) shows that both samples have similar wind speeds and rotational speeds at 5.5 m/s; the D1 Normal and D1 Upside down turbines have rotational speeds of 790 and 750 RPM, respectively.

Turbine performance using blade D4 Normal is better than the other types. This is due to the low turbulence that occurs. This small intensity of turbulence reduces the formation of vortices downstream of the blade, so the flow that occurs behind the blade is smooth. This phenomenon causes an increase in turbine rotation, which will be linear with an increase in wind speed [16].

The angle of attack of the VAWTs blades played a dominant role in the production of the aerodynamic power and the power production of the turbine. The proposed method can decrease the Root Mean Square Error (RMSE) by as much as approximately 33.8% for the three tested air flow velocities slackened to small wind turbine conditions [19]. The twisted blade rotor design not only enhances the power coefficient but also enables the self-starting ability. However, the blades generated slightly higher thrust for the load [20]. The twisted blades achieve a higher static torque coefficient over the whole revolution that in turn augments the self-starting capabilities of the blades [21].

Figure 11 shows the VAWT model and the cut-in speed of 3 Blades with AR=1.5, 3 Blades with AR=1.0, 4 Blades with AR=1.5 and 4 Blades with AR=1.0 with varying twist and attack angles. It was found that the 4 Blades with AR=1.5 and 4 Blades AR=1.0 had lower cut-in speeds than the others, at about 1.70 to 1.80 m/s wind speed. The 4 Blades with AR=1.5 showed the best lower cut-in at 1.70 m/s operated under the angles of (0° Twist, -30° Attack), (60° Twist, 0° Attack), (60° Twist, 30° Attack) and (60° Twist, 60° Attack). Meanwhile, the 4 Blades with AR=1.0 achieved the best lower cut-in at 1.70 m/s operating under the angles of (0° Twist, -30° Attack), (60° Twist, 30° Attack) and (60° Twist, 60° Attack). However, the conditions of angles at (120° Twist, 30° Attack), (120° Twist, 60° Attack) and (120° Twist, 90° Attack) could not be installed on the plate because of the highly tortuous angles of the blades which would result in insufficient surface area.

Additionally, the 3 Blades with AR=1.5 operated with lower cut-in than the 3 Blades with AR=1.0. The 3 Blades with AR=1.5 cut in at 1.75 – 2.10 m/s, with the best lower cut-in at 1.75 m/s which occurred under the angle of (120° Twist, 30° Attack). Meanwhile, the 3 Blades with AR=1.0 cut in at 2.10 – 2.40 m/s, exhibiting the best lower cut-in at 2.10 when operating under the angles of (60° Twist, 0° Attack), (60° Twist, 60° Attack), (120° Twist, 30° Attack), (120° Twist, 60° Attack) and (120° Twist, 90° Attack). The number of blades can affect the generation of torque, with the 4 blades rating higher than 3 blades [22]. The helical savonius blade angle affected the average power efficient

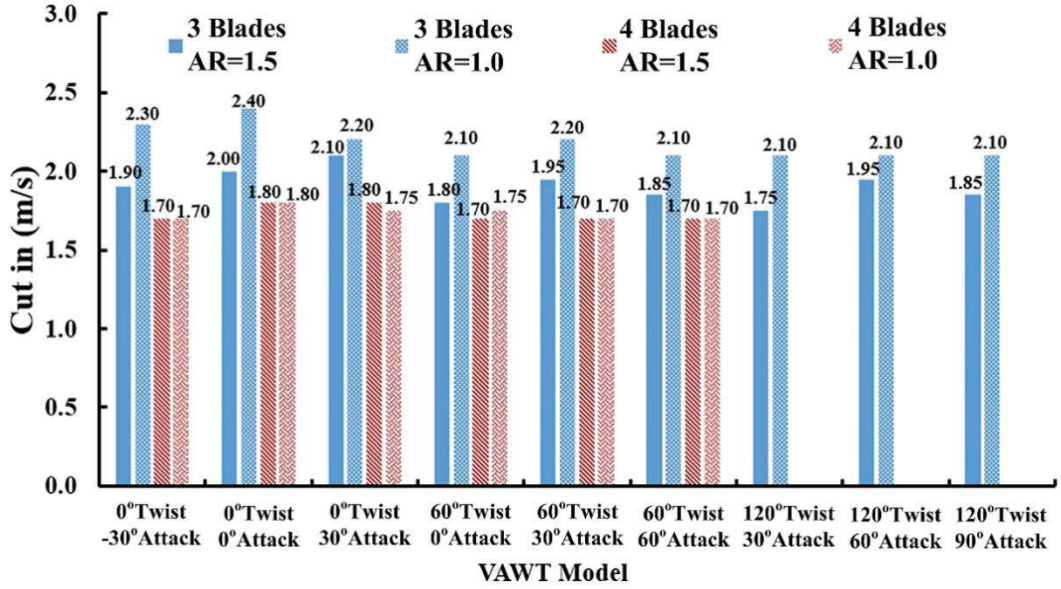

Figure. 11 VAWT model and cut-in wind speed of 3 Blades with AR=1.5, 3 Blades with AR=1.0, 4 Blades with AR=1.5 and 4 Blades with AR=1.0 that were varied the Twist and Attack angle of VAWT Model.

Figure 12. The 15 kW wind turbine pole was installed in Krabi province, Thailand. This wind turbine used the 3 blades with AR=1.5, operating with cut-in at 1.75 m/s that acted under the angles of 120° Twist and 30° Attack.

(Cp), but this depends on the angles of the blades which transfer wind speed to power [23].

Finally, the model of 3 blades with AR=1.5 operating with cut-in at 1.75 m/s which operated under the angles of 120° Twist and 30° Attack was fabricated as a 15 kW wind turbine which was installed in Krabi province, Thailand. This wind turbine combined 54 wind turbines connected to 300 W electrical generators. The combination of 54 turbines took the form of a beautiful wind tree turbine which can produce electrical power for the grid of the Provincial Administrative Organization.

CONCLUSION

The Dipterocarpus alatus has been used to design effective airfoil blades that can be duplicated for use in vertical

axis wind turbine blades. The D1 and D4 were the original structures of Dipterocarpus alatus that could be turned counter-clockwise with greater efficiency than the alternatives. According to the experiment, D1 Normal has a rotating speed of 180 RPM and a minimum wind speed of 1.5 m/s. Therefore, the VAWT model was based on the D1 structure fabricated from acrylic materials at 3 mm thickness (0.9 m high x 0.9 m diameter). This design used both 3 blades and 4 blades and aspect ratios (AR) of 1.5 and 1.0.

The results indicated that the 4 Blades with AR=1.5 showed the best lower cut-in at 1.70 m/s operating under the angles of (0° Twist, -30° Attack), (60° Twist, 0° Attack), (60° Twist, 30° Attack) and (60° Twist, 60° Attack). Meanwhile, the 4 Blades with AR=1.0 achieved the best lower cut-in at 1.70 m/s operating under the angles of (0° Twist, -30° Attack), (60° Twist, 30° Attack) and (60° Twist, 60° Attack).

Meanwhile, the 3 Blades with AR=1.5 operated with a clearly lower cut-in than the 3 Blades with AR=1.0. The 3 Blades with AR=1.5 cut in at 1.75 – 2.10 m/s, with the best lower cut-in at 1.75 m/s operating under the angle of (120° Twist, 30° Attack). In comparison, the 3 Blades with AR=1.0 cut in at 2.10 – 2.40 m/s, with the best lower cut-in at 2.10 operating under numerous angles of (60° Twist, 0° Attack), (60° Twist, 60° Attack), (120° Twist, 30° Attack), (120° Twist, 60° Attack) and (120° Twist, 90° Attack). The conditions of the VAWT blades affecting the efficiency included AR, number of blades and the tortuous blade angle. The interesting model is the one with 3 Blades and AR=1.5 with the operating cut-in at 1.75 m/s under the angle of (120° Twist, 30° Attack) since it delivered high torque at low speed, and low cost. Therefore, the biomimicry duplicating Dipterocarpus alatus has the potential to be used for producing VAWT blades.

ABBREVIATIONS

VAWTs	Vertical axis wind turbines
HAWTs	Horizontal axis wind turbines
RPM	Revolutions per minute
AR	Aspect ratio
LET	Leading edge tubercles
LEV	Leading edge vortices
DTU	Danmarks Tekniske Universitet
EPS	Expandable polystyrene
ϕ	The angle of the relative wind
α	The angle of attack
θ	The angular frequency of rotational shaft
β	Twist angle
f	Frequency
L	Lift components
D	Drag components
F_L	Lift force
F_D	Drag force
F_G	Gravitational force
C_L	Lift coefficients
C_D	Drag coefficients
v	The relative wind velocity at the blade
λ	Constant value
m	Mass
g	Acceleration due to gravity
A	The area of the blades of Dipterocarpus alatus
ρ	The air density (approximately 1.225 kg/m^3)
H	Height
D	Dimension
$D_{1\text{-}5}$	1 to 5 Dipterocarpus alatus model
RMSE	Root Mean Square Error

ACKNOWLEDGEMENTS

This investigation was suppoted by 2019 PSU funding (ENV620167S).

AUTHORSHIP CONTRIBUTIONS

Authors equally contributed to this work.

DATA AVAILABILITY STATEMENT

The authors confirm that the data that supports the findings of this study are available within the article. Raw data that support the finding of this study are available from the corresponding author, upon reasonable request.

CONFLICT OF INTEREST

The author declared no potential conflicts of interest with respect to the research, authorship, and/or publication of this article.

ETHICS

There are no ethical issues with the publication of this manuscript.

STATEMENT ON THE USE OF ARTIFICIAL INTELLIGENCE

Artificial intelligence was not used in the preparation of the article.

REFERENCES

[1] Wang Z, Zhuang M. Leading-edge serrations for performance improvement on a vertical-axis wind turbine at low tip-speed-ratios. Appl Energy 2017;208:1184–1197. [CrossRef]

[2] Wang Z, Wang Y, Zhuang M. Improvement of the aerodynamic performance of vertical axis wind turbines with leading-edge serrations and helical blades using CFD and Taguchi method. Energy Convers Manag 2018;177:107–121. [CrossRef]

[3] Zhao Z, Wang D, Wang T, Shen W, Liu H, Chen M. A review: Approaches for aerodynamic performance improvement of lift-type vertical axis wind turbine. Sustain Energy Technol Assess 2022;49:101789. [CrossRef]

[4] Saeidi D, Sedaghat A, Alamdari P, Alemrajabi AA. Aerodynamic design and economical evaluation of site specific small vertical axis wind turbines. Appl Energy 2013;101:765–775. [CrossRef]
[5] Kumar R, Raahemifar K, Fung AS. A critical review of vertical axis wind turbines for urban applications. Renew Sustain Energy Rev 2018;89:281–291. [CrossRef]
[6] Guven AF, Yorukeren N. A comparative study on hybrid GA-PSO performance for stand-alone hybrid energy systems optimization. Sigma J Eng Nat Sci 2024;42:1410–1438. [CrossRef]
[7] Chen WH, Chen CY, Huang CY, Hwang CJ. Power output analysis and optimization of two straight-bladed vertical-axis wind turbines. Appl Energy 2017;185:223–232. [CrossRef]
[8] Kc A, Whale J, Urmee T. Urban wind conditions and small wind turbines in the built environment: A review. Renew Energy 2019;131:268–283. [CrossRef]
[9] Balduzzi F, Bianchini A, Carnevale EA, Ferrari L, Magnani S. Feasibility analysis of a Darrieus vertical-axis wind turbine installation in the rooftop of a building. Appl Energy 2012;97:921–929. [CrossRef]
[10] Ngoc DM, Techato K, Niem LD, Yen NT, Dat NV, Luengchavanon M. A Novel 10 kW Vertical Axis Wind Tree Design: Economic Feasibility Assessment. Sustain 2021;13. [CrossRef]
[11] Trongtorkarn M, Theppaya T, Techato K, Luengchavanon M, Kasagepongsarn C. Relationship between Starting Torque and Thermal Behaviour for a Permanent Magnet Synchronous Generator (PMSG) Applied with Vertical Axis Wind Turbine (VAWT). Sustain 2021;13:9151. [CrossRef]
[12] Ahmad M, Zafar MH. Enhancing vertical axis wind turbine efficiency through leading edge tubercles: A multifaceted analysis. Ocean Eng 2023;288:116026. [CrossRef]
[13] Wang-yu L, Zhang Y. Network study of plant leaf topological pattern and mechanical property and its application. Adv Nat Sci 2010;3:82–92.
[14] Momeni F, Sabzpoushan S, Valizadeh R, Morad MR, Liu X, Ni J. Plant leaf-mimetic smart wind turbine blades by 4D printing. Renew Energy 2019;130:329–351. [CrossRef]
[15] Mishnaevsky L, Jafarpour M, Krüger J, Gorb SN. A New Concept of Sustainable Wind Turbine Blades: Bio-Inspired Design with Engineered Adhesives. Biomimetics 2023;8:448. [CrossRef]
[16] Seidel C, Jayaram S, Kunkel L, Mackowski A. Structural Analysis of Biologically Inspired Small Wind Turbine Blades. Int J Mech Mater Eng 2017;12:19. [CrossRef]
[17] Lentink D, Dickson WB, Leeuwen JLV, Dickinson MH. Leading-edge vortices elevate lift of autorotating plant seeds. Science 2009;324:1438–1440. [CrossRef]
[18] Eadkong T, Pimton P, Dam OP, Channuie P. Unraveling the vertical motion of Dipterocarpus alatus seed using Tracker. Phys Scr 2020;95:055003. [CrossRef]
[19] Elsakka MM, Ingham DB, Ma L, Pourkashanian M. CFD analysis of the angle of attack for a vertical axis wind turbine blade. Energy Convers Manag 2019;182:154–165. [CrossRef]
[20] Saad AS, El-Sharkawy II, Ookawara S, Ahmed M. Performance enhancement of twisted-bladed Savonius vertical axis wind turbines. Energy Convers Manag 2020;209:112673. [CrossRef]
[21] Saad AS, Elwardany A, El-Sharkawy II, Ookawara S, Ahmed M. Performance evaluation of a novel vertical axis wind turbine using twisted blades in multi-stage Savonius rotors. Energy Convers Manag 2021;235:114013. [CrossRef]
[22] Adeyeye KA, Ijumba N, Colton J. The effect of the number of blades on the efficiency of a wind türbine. IOP Conf Ser Earth Environ Sci 2021;012020. [CrossRef]
[23] Kamal MM, Abbas A, Alam T, Gupta NK, Khargotra R. Hybrid cross-flow hydrokinetic turbine: Computational analysis for performance characteristics with helical Savonius blade angle of 135°. Results Eng 2023;20:101610. [CrossRef]